

Topological lens effects in universes with non-euclidean compact spatial sections

R. Lehoucq¹, J.-P. Luminet², and J.-Ph. Uzan^{3,2}

¹ CE-Saclay, DSM/DAPNIA/Service d’Astrophysique, F-91191 Gif sur Yvette cedex, France (roller@discovery.saclay.cea.fr)

² Département d’Astrophysique Relativiste et de Cosmologie, Observatoire de Paris, CNRS–UPR 176, F-92195 Meudon, France (Jean-Pierre.Luminet@obspm.fr)

³ Département de Physique Théorique, Université de Genève, 24 quai E. Ansermet, CH-1211 Geneva, Switzerland (uzan@amorgos.unige.ch)

Received 17 November 1998 / Accepted 8 January 1999

Abstract. Universe models with compact spatial sections smaller than the observable universe produce a topological lens effect. Given a catalog of cosmic sources, we estimate the number of topological images in locally hyperbolic and locally elliptic spaces, as a function of the cosmological parameters, of the volume of the spatial sections and of the catalog depth. Next we apply the crystallographic method, aimed to detect a topological signal in the 3D distance histogram between images, to compact hyperbolic models. Numerical calculations in the Weeks manifold allow us to check the absence of crystallographic signature of topology, due to the fact that the number of copies of the fundamental domain in the observable covering space is low and that the points are not moved the same distance by the holonomies of space.

Key words: cosmology: theory – cosmology: large-scale structure of Universe

1. Introduction

The question of whether our universe has a finite spatial extension or not is still an open question related to its topology (see Lachièze-Rey & Luminet 1995 for a review and the proceedings of the workshop *Cosmology and topology* 1998 for latest developments). Recently, there has been a large activity to constrain and/or to observe the shape and the size of the universe. Many methods have been proposed to detect its spatial topology using catalogs of discrete sources like clusters of galaxies (Lehoucq et al. 1996) and quasars (Roukema 1996, 1997) or the cosmic microwave background (Stevens et al. 1993, de Oliveira Costa et al. 1996, Cornish et al. 1998a,b,c, Uzan 1998a,b). All the methods rest on a “topological lens” effect which generates multiple images of cosmic sources, as soon as the compact spatial sections have a volume smaller than the observable universe. In the past, the idea of using the topological images was extensively applied to universe models with Euclidean (see e.g. Fang & Sato 1983, Demianski & Lapucha 1987, Fagundes & Wichoski 1987, Ellis 1971) and hyperbolic (see e.g. Gott 1980) spatial

sections. More recently, the crystallographic method (Lehoucq et al. 1996), which relies on the existence of topological images whatever the underlying geometry, was applied only to locally flat universes, and was able to put a bound on the characteristic size L of Euclidean space to $L \leq 650 h^{-1}$ Mpc (h being the Hubble constant in units of 100 km/s/Mpc). The efficiency of the crystallographic method obviously depends on the number of topological images of a given object within the horizon size or within the limits of current catalogs used for the test. The applicability of the method in Euclidean space has also been discussed by Fagundes & Gausmann (1997) when the size of the physical space is comparable to the horizon size.

We can naturally wonder if the method applies as well in locally hyperbolic or elliptic manifolds, and if we can get any constraint on the size of space from the existing catalogs of cosmic objects. We keep also in mind the growing weight of observational evidence for a low density universe (see e.g. Spergel 1998). Thus in this article we focus mainly on universes with locally hyperbolic compact spatial sections (Thurston 1979, 1997). The universe is described by a 4-manifold \mathcal{M} and a Lorentzian metric g and we assume that \mathcal{M} can be splitted as $\mathcal{M} = \Sigma \times \mathbb{R}$ (see e.g. Hawking & Ellis 1973 for the conditions of such a splitting). As any multi-connected closed three-dimensional manifold, Σ can be described by its fundamental domain (a polyhedron) and its holonomy group Γ , which identifies the faces of the polyhedron by pairs (Lachièze-Rey & Luminet 1995). Such hyperbolic manifolds $\Sigma = H^3/\Gamma$ have a remarkable property that links topology and geometry: the *rigidity theorem* (Mostow 1973, Prasad 1973) implies that geometrical quantities such as the volume, the lengths of its closed geodesics, . . . , are topological invariants. The volume can then be used to classify these manifolds (Thurston 1979, 1997). The volumes of compact hyperbolic manifolds are bounded below (Gabai et al. 1996) by $\text{Vol}_{\min} \simeq 0.166$, in units of the curvature radius.

The smallest known compact hyperbolic manifold, likely to produce the greatest topological lens effects, is the Weeks space (Weeks 1985, Matveev & Fomenko 1988, see Appendix A for a description), such that $\text{Vol} = 0.94272$, $r_+ = 0.7525$, $r_- = 0.5192$, where r_+ and r_- are respectively the radii of the

Send offprint requests to: R. Lehoucq

largest (smallest) geodesic ball that contains (is contained in) the fundamental domain.

The fundamental domain and the holonomy group of the known three-dimensional compact hyperbolic manifolds can be found by using the software *SnapPea* written by Weeks (<http://www.geom.umn.edu:80/software>) which gives all the information needed to compute the topological lens effects, such as the volume, the generators of the holonomy group, the lengths of closed geodesics.

Fagundes (1993) already used a universe whose spatial sections had the topology of the Weeks manifold to discuss the controversy about the quasars redshifts. In his paper, he gave an interesting description of the fundamental domain and of the holonomy group. The same author previously studied a 2+1 hyperbolic cosmology (Fagundes 1985) and a universe with hyperbolic spatial sections whose fundamental domain was a hyperbolic icosahedron (Fagundes 1989, 1990), known as the Best space (Best 1971), to investigate the same problem.

In Sect. 2 we describe the crystallographic method and the way to implement it, focusing on the interface with *SnapPea*. Sect. 3 is devoted to the applicability of this method to compact hyperbolic universes (Sect. 3.1) and to compact elliptic universes (Sect. 3.2) and specially the dependence of the number of images as a function of the density parameter and of the cosmological constant. Numerical results of simulations in the Weeks manifold are given in Sect. 4, and we discuss the influence of the catalog, of the density parameter and of the position of the observer within the fundamental domain.

2. The crystallographic method in compact hyperbolic universes

In this section, we describe the crystallographic method and the way to implement it to universes with compact hyperbolic spatial sections. The local geometry of such a universe is described by a Friedmann-Lemaître metric

$$ds^2 = -dt^2 + a^2(t) (d\chi^2 + \sinh^2 \chi d\Omega^2). \quad (1)$$

where a is the scale factor, t the cosmic time and $d\Omega^2 \equiv d\theta^2 + \sin^2 \theta d\varphi^2$ the infinitesimal solid angle.

A locally hyperbolic three-dimensional manifold can be embedded in a four-dimensional Minkowski space by introducing the set of coordinates $(x^\mu)_{\mu=0..3}$ related to the intrinsic coordinates (χ, θ, φ) through (see e.g. Wolf 1984, Coxeter 1965)

$$\begin{aligned} x_0 &= \cosh \chi \\ x_1 &= \sinh \chi \sin \theta \sin \varphi \\ x_2 &= \sinh \chi \sin \theta \cos \varphi \\ x_3 &= \sinh \chi \cos \theta, \end{aligned} \quad (2)$$

so that the three-dimensional hyperboloid H^3 has the equation

$$-x_0^2 + x_1^2 + x_2^2 + x_3^2 = -1. \quad (3)$$

[Note that when $a(t) = t$, the line element (1) describes a Milne universe which, using the coordinates transformation

$(t' = t \cosh \chi, r = t \sinh \chi)$ reduces to the Minkowski line element in spherical coordinates. This can describe a $\Omega = 0$ open cosmology (see e.g. Misner et al. 1973).]

With these notations, the comoving spatial distance between two points of comoving coordinates x and y can be computed directly in the Minkowski space by (Fagundes 1989, 1990)

$$\text{dist}[x, y] = \arg \cosh \left[\frac{x^\mu y_\mu}{(x^\mu x_\mu)^{1/2} (y^\mu y_\mu)^{1/2}} \right], \quad (4)$$

where $x_\mu = \eta_{\mu\nu} x^\nu$, $\eta_{\mu\nu}$ being the Minkowskian metric. Note that Minkowski space can be mapped onto the interior of an ordinary sphere S^2 of unit radius by using the Klein coordinates $(X_i)_{i=1..3}$ (Wolf 1984, Coxeter 1965) defined by

$$X_i = x_i/x_0. \quad (5)$$

The universal covering space being described, we now choose a topology, i.e. a holonomy group Γ such that the spatial sections are $\Sigma = H^3/\Gamma$. Σ can be described by its fundamental domain whose $2K$ faces are identified by pairs by the elements of Γ . Γ has $2K$ generators which, in the case of the Weeks manifold ($K = 9$) can be obtained from *SnapPea* and are given in Appendix A.

Indeed, the elements of Γ are isometries so that

$$\forall (x, y) \in \Sigma \quad \forall g \in \Gamma, \quad \text{dist}[x, y] = \text{dist}[g(x), g(y)]. \quad (6)$$

The crystallographic method (Lehoucq et al. 1996) is based on a property of multi-connected universes according to which each topological image of a given object is linked to each other one by the holonomies of space. Indeed, we do not know these holonomies as far as we have not determined the topology, but we know that they are isometries. For instance in locally Euclidean universes, to each holonomy is associated a distance λ , equal to the length of the translation by which the fundamental domain is moved to produce the tessellation in the covering space. Assume the fundamental domain contains N objects (e.g. galaxy clusters), if we calculate the mutual 3D distances between every pair of topological images (inside the particle horizon), the distances λ will occur N times for each copy of the fundamental domain, and all other distances will be spread in a smooth way between zero and two times the horizon distance. In a histogram plotting the number of pairs versus their 3D separations, the distances λ will thus produce peaks. Simulations indeed showed that the pairs between two topological images of the same object drastically emerge from ordinary pairs (Lehoucq et al. 1996) in the histogram.

Two kind of catalogs of astronomical objects can be thought of to apply this method: the galaxy cluster catalogs, which typically have a redshift depth $z = 1$, and the quasars catalogs, which typically extend to $z = 3$. Concerning quasars, even if their lifetime is probably too short for them to be good candidates for producing topological images, they are usually part of systems that have a much larger lifetime (Paál 1971). The angular resolution needed is given by the fact that the objects have a peculiar velocity and that they will not be seen at exactly the same position (Lachièze-Rey & Luminet 1995). Note that

the crystallographic method, contrary to the “direct” method which would try to recognize topological images of individual objects, is not plagued by the evolution problem, i.e. that topological images of the same object are seen at different stages of its evolution.

3. Estimation of the number of topological images in non-Euclidean universes

3.1. Compact hyperbolic universes

To estimate the applicability of the crystallographic method in hyperbolic compact universes, we estimate the number of topological images of a given object up to a redshift z . With the metric (1), the Einstein equations reduce to the Friedmann equation

$$H^2 = \kappa \frac{\rho_m}{3} - \frac{K}{a^2} + \frac{\Lambda}{3}, \quad (7)$$

ρ_m being the matter density, Λ the cosmological constant and $\kappa \equiv 8\pi G/c^4$. H is the Hubble constant defined by $H \equiv \dot{a}/a$ with $\dot{X} \equiv \partial_t X$. We choose the units such that the curvature index is $K = -1$. Introducing $\Omega_\Lambda \equiv \Lambda/3H^2$, $\Omega_m \equiv \kappa\rho_m/3H^2$ and the redshift z defined by $1+z \equiv a_0/a$, Eq. (7) can be rewritten as (see e.g. Peebles 1993)

$$\frac{H^2}{H_0^2} = \Omega_{m0}(1+z)^3 + \Omega_{\Lambda0} + (1 - \Omega_{m0} - \Omega_{\Lambda0})(1+z)^2. \quad (8)$$

For that purpose we have used Eq. (7) evaluated today (i.e. at $t = t_0$) and we have assumed that we were in a matter dominated universe so that $\rho_m \propto a^{-3}$ [this hypothesis is very good since we restrict ourselves to small redshift].

The radius of the observable region at a redshift z is given by integration of the radial null geodesic equation $d\chi = dt/a$ and reads

$$\begin{aligned} \chi(z) &\equiv \int_{a_0}^a \frac{da}{a\dot{a}} \\ &= \int_{\frac{1}{1+z}}^1 \frac{\sqrt{1 - \Omega_{m0} - \Omega_{\Lambda0}} dx}{x \sqrt{\Omega_{\Lambda0}x^2 + (1 - \Omega_{m0} - \Omega_{\Lambda0}) + \Omega_{m0}/x}}. \end{aligned} \quad (9)$$

This equation is integrated numerically and the result can be compared, when $\Omega_\Lambda = 0$, to the analytic expression (see e.g. Gradshteyn & Ryzhik 1980)

$$\chi(z) = \left[\arg \cosh \left(1 + \frac{2(1 - \Omega_{m0})}{\Omega_{m0}} x \right) \right]_{1/1+z}^1. \quad (10)$$

The number of topological images of a given object at a redshift z can be estimated by computing the ratio between the volume of the geodesic sphere of radius $\chi(z)$ and the volume of the manifold which is a topological invariant. This leads to

$$N(\Omega_{m0}, \Omega_{\Lambda0}; z < Z) = \frac{\pi (\sinh 2\chi(Z) - 2\chi(Z))}{\text{Vol}(\Sigma)}. \quad (11)$$

It can be easily understood that this under-estimates the number of images.

As seen on Fig. 1, detecting the topology with clusters of galaxies would require both $\Omega_{\Lambda0}$ and Ω_{m0} to be very low. The

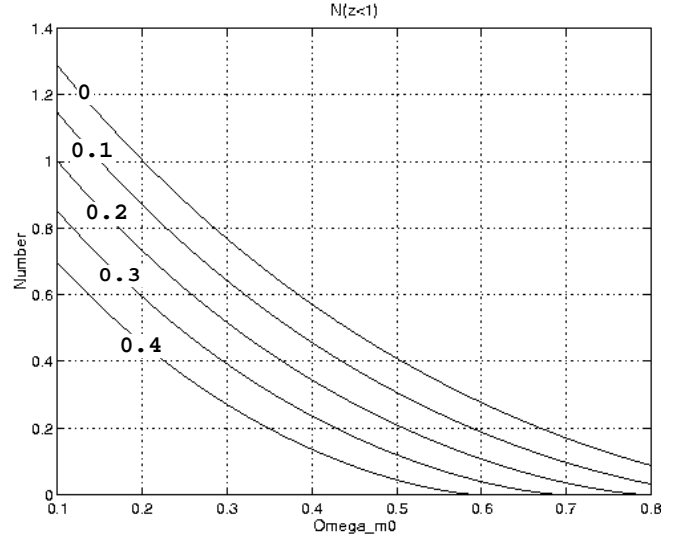


Fig. 1. Number of topological images in a catalog of clusters up to a redshift $z = 1$ as a function of Ω_{m0} and $\Omega_{\Lambda0}$ in a universe whose spatial sections have the topology of the Weeks manifold. The curves are labeled by the values of $\Omega_{\Lambda0}$. Topology is detectable only if the number of topological images is greater than unity.

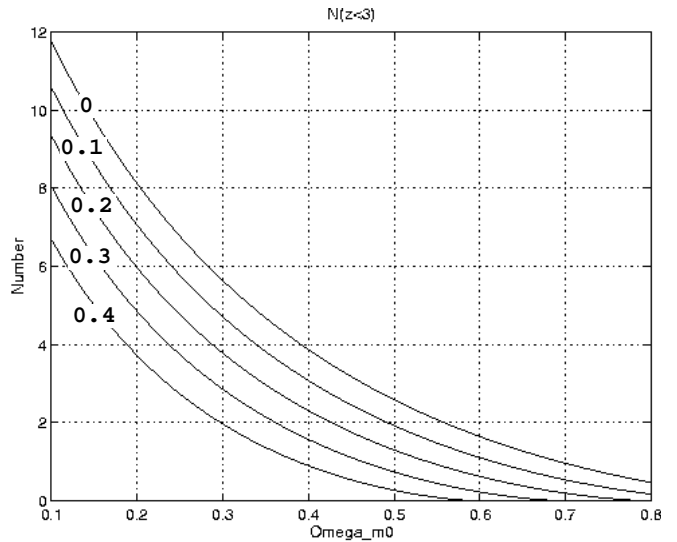


Fig. 2. The same as Fig. 1 in the case of a catalog of quasars extending up to a redshift $z = 3$.

situation is much better with groups of quasars (Fig. 2). Fig. 3 shows the effect of the two parameters (Ω_Λ , Ω_m) on the number of topological images inside the observable universe. This also provides an estimation of the number of expected matched circles in the circle method (Cornish 1998a,b,c).

Given standard values of the cosmological parameters (Proceedings of the “XXIIIrd rencontres de Moriond”), the numbers of pairs involving an object and one of its topological images will be statistically low in compact hyperbolic universes. For instance a cluster catalog will give no signature whatever the parameters and a quasar catalog will typically require the cosmological constant to vanish and the density parameter to be

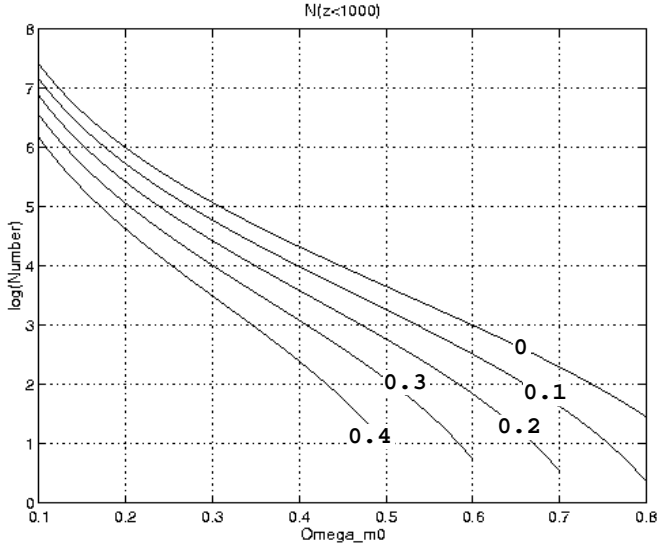


Fig. 3. Number of topological images within the observable universe (i.e. with $z < 1000$) in function of Ω_{m0} and $\Omega_{\Lambda0}$. This estimates the number of expected matched circles on the cosmic microwave background.

$\Omega_{m0} < 0.4$. It can also be seen that the generic effect of the cosmological constant is to make the horizon volume bigger and thus to dilute the number of topological images.

3.2. Compact elliptic universes

We proceed as in the previous section but now the spatial sections are of the form S^3/Γ , where the holonomy group Γ is either a cyclic group, a dihedral group or the symmetry groups T , O , I respectively of the tetrahedron, octahedron or isocahedron (see Lachièze-Rey & Luminet 1995 for a complete description). The local geometry of the background spacetime is described by a Friedmann-Lemaître universe with the metric

$$ds^2 = -dt^2 + a^2(t) (d\chi^2 + \sin^2 \chi d\Omega^2). \quad (12)$$

In units of the curvature radius (i.e. when $K = +1$), the volume of the spatial sections is given by

$$\text{Vol}(S^3/\Gamma) = \frac{\text{Vol}(S^3)}{|\Gamma|} = \frac{2\pi^2}{|\Gamma|}, \quad (13)$$

where $|\Gamma|$ is the order of the group Γ (e.g. $|\Gamma| = 12, 24, 60$ respectively for T, O, I ; Lachièze-Rey & Luminet 1995, Wolf 1984). Since the volume of the sphere of radius χ is given by

$$\text{Vol}(\chi) = \frac{2\chi - \sin 2\chi}{2\pi}, \quad (14)$$

the number of topological images defined as in Sect. 3.1, is

$$N(\Omega_{m0}, \Omega_{\Lambda0}; z < Z) = \frac{|\Gamma|}{2\pi} (2\chi(Z) - \sin 2\chi(Z)). \quad (15)$$

$\chi(Z)$ is computed as in Eqs. (8-9) by changing the sign of the curvature index K in Eq. (7) [note that it does not affect Eq. (8)] so that

$$\chi(z) = \int_{\frac{1}{1+z}}^1 \frac{\sqrt{\Omega_{m0} + \Omega_{\Lambda0} - 1} dx}{x \sqrt{\Omega_{\Lambda0} x^2 + (1 - \Omega_{m0} - \Omega_{\Lambda0}) + \Omega_{m0}/x}}. \quad (16)$$

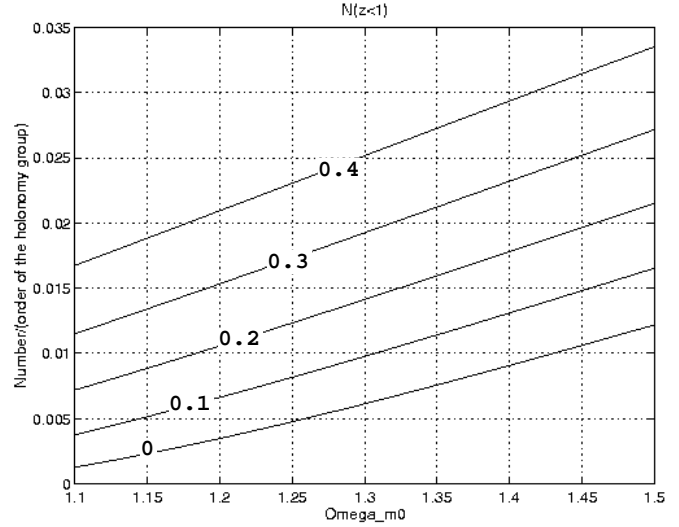


Fig. 4. Number of topological images in a galaxy cluster catalog up to a redshift $z = 1$ in function of Ω_{m0} and $\Omega_{\Lambda0}$ in a locally elliptic space.

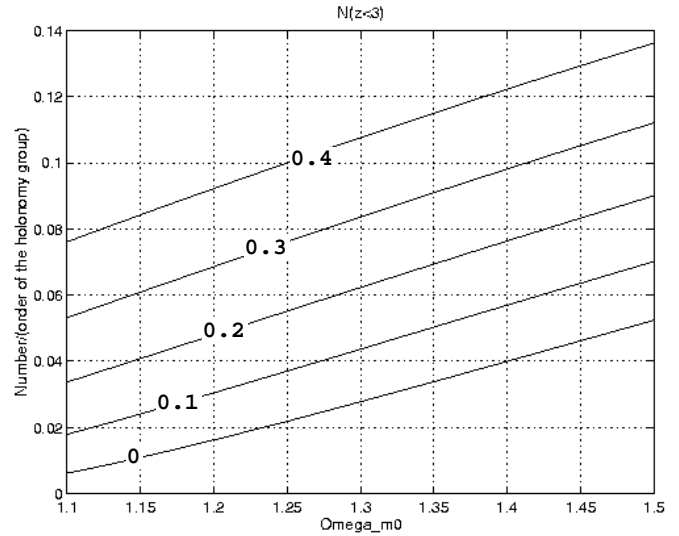


Fig. 5. Same as Fig. 4 for a catalog of quasars up to a redshift $z = 3$.

When $\Omega_{\Lambda} = 0$, this expression can be computed analytically, as in Eq. (10) (Peebles 1993).

We plot $N/|\Gamma|$ in term of Ω_{m0} for different values of $\Omega_{\Lambda0}$. It can be concluded that the topology of an elliptic space can be detected respectively by a catalog of galaxy clusters (see Fig. 4) only if $|\Gamma| > 200$ and if $|\Gamma| > 50$ in a catalog of quasars (see Fig. 5) when $\Omega_{\Lambda} = 0$.

A non vanishing cosmological constant improves the situation and holonomy groups of lower order can be considered. Nevertheless, we are still constrained by the fact that the total energy density has to be compatible with the estimated age of the universe.

4. Numerical results

In our numerical simulations, we concentrate only on compact hyperbolic models. We first generate an idealised catalog, \mathcal{C} , by

distributing *homogeneously* objects in the fundamental domain. A homogeneous distribution is defined by the requirement that the number of objects per unit volume dN/dV is constant, dV being given by

$$\begin{aligned} dV &= \sinh^2 \chi d\chi \sin \theta d\theta d\varphi \\ &= d[\cosh 2\chi - 2\chi] d \cos \theta d\varphi, \end{aligned} \quad (17)$$

with $\cos \theta \in [-1, 1]$ and $\varphi \in [-\pi, \pi]$. We first create a catalog in the smallest sphere containing the fundamental polyhedron. Then, in order to obtain a set \mathcal{C}_1 , we reject the points lying outside the fundamental domain by checking if they are on the same side of the faces of the fundamental domain than its center. This can easily be achieved when we know the Minkowskian coordinates of the vertices of the polyhedron, which can be obtained from *SnapPea* (see Appendix A).

We then unfold the catalog by applying the generators of the holonomy group to obtain the set \mathcal{C}_2

$$\mathcal{C}_2 = \left\{ \tilde{x}, \forall x \in \mathcal{C}_1, \quad \tilde{x} = \sum_{g \in \Gamma} g(x); \quad \chi(\tilde{x}) \leq \chi_m \right\}, \quad (18)$$

where χ_m is the maximal value of the radial coordinate of the set \mathcal{C}_2 . To generate a catalog with a given depth z in redshift, we truncate \mathcal{C}_2 so that

$$\mathcal{C}(z) = \{x \in \mathcal{C}_2; \quad \text{dist}[0, x] \leq \chi(\Omega_{m0}, \Omega_{\Lambda0}; z)\}, \quad (19)$$

where $\chi(\Omega_{m0}, \Omega_{\Lambda0}; z)$ is given by Eq. (9). This accounts as selecting the objects located within the geodesic ball of radius $\chi(\Omega_{m0}, \Omega_{\Lambda0}; z)$ centered onto an observer placed at the centre. We then compute all the three dimensional separations between all the pairs of $\mathcal{C}(z)$ and plot the histogram of the number of pairs with a given separation.

Indeed the former procedure applies when the observer stands at the center of the polyhedron ($\chi = 0$). Now, if the observer is at a position, ($\chi_{\oplus} \neq 0, \theta_{\oplus} = 0, \varphi_{\oplus} = 0$) say, we have to perform a coordinate change to center the catalog on the observer before selecting the object as in Eq. (19). The Minkowskian coordinates, x' say, of a point in the frame centered on the observer are related to the “old” coordinates x (i.e. in the frame centered on $\chi = 0$) by

$$x' = \mathcal{M}_{0 \rightarrow \oplus} x \quad \text{with} \quad \det(\mathcal{M}_{0 \rightarrow \oplus}) = 1, \quad (20)$$

where $\mathcal{M}_{0 \rightarrow \oplus}$ is a matrix determined by the fact that the image of the “old” center $\chi = 0$ is the observer’s position $x_{\oplus} = (\cosh \chi_{\oplus} \equiv \gamma, 0, 0, \sinh \chi_{\oplus} \equiv \beta\gamma)$ so that

$$\mathcal{M}_{0 \rightarrow \oplus} = \begin{pmatrix} \gamma & 0 & 0 & -\beta\gamma \\ 0 & 1 & 0 & 0 \\ 0 & 0 & 1 & 0 \\ -\beta\gamma & 0 & 0 & \gamma \end{pmatrix}. \quad (21)$$

We recognize a Lorentz transformation. The same method applies when $\theta_{\oplus} \neq 0$ and $\varphi_{\oplus} \neq 0$ but the matrices are not so straightforward, so that we do not consider them here. The catalog $\mathcal{C}(z)$ is then constructed as in Eq. (19) but using the points

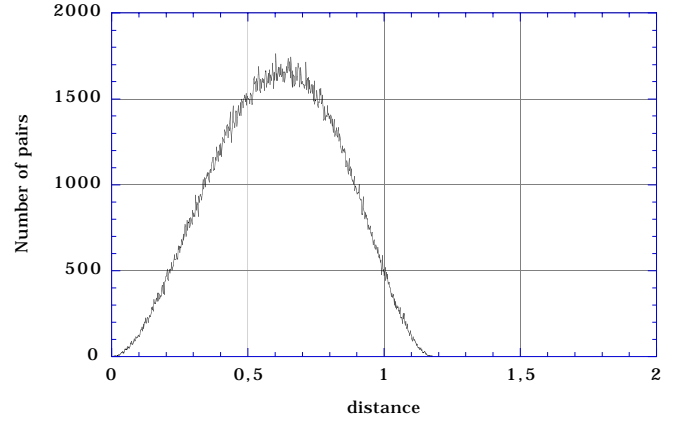


Fig. 6. Pair histogram for a galaxy cluster catalog ($z = 1$) measured by an observer centered in $\chi = 0$ in a hyperbolic universe whose spatial sections have the topology of the Weeks manifold and $\Omega_{m0} = 0.2$; $\Omega_{\Lambda} = 0$.

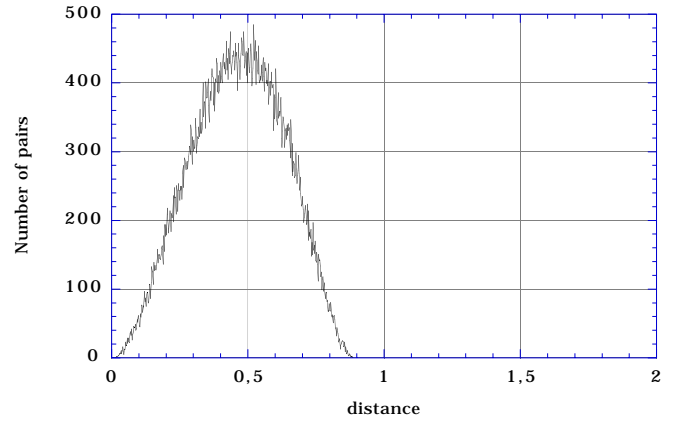


Fig. 7. Pair histogram for a galaxy cluster catalog ($z = 1$) measured by an observer centered in $\chi = 0$ in a universe whose spatial sections have the topology of the Weeks manifold and $\Omega_{m0} = 0.5$.

x' instead of x , and the procedure of pair computation is not affected.

We now generate some pair histograms in a universe whose spatial sections have the topology of the Weeks manifold using $N = 1000$ objects in the fundamental domain. In Fig. (6) we assume that $\Omega_{\Lambda} = 0$, $\Omega_{m0} = 0.2$, that the observer stands at the center of the polyhedron ($\chi = 0$) and that he uses a galaxy cluster catalog of depth $z = 1$. We then study the dependence on Ω_{m0} (see Fig. 7 where $\Omega_{m0} = 0.5$), on the position of the observer (see Fig. 8 where the observer stands near a face) and on the catalog depth (see Fig. 9 where we assume that the observer is using a quasar catalog of depth $z = 3$).

As a matter of fact, we do not observe any peaks in these histograms, contrarily to the case of locally Euclidean universes. Let us try to understand why. Two kinds of pairs can give birth to peaks (see Fig. 10):

- *Type I pairs* of the form $\{g(x), g(y)\}$ since for all points and all elements g of Γ , $\text{dist}[g(x), g(y)] = \text{dist}[x, y]$.
- *Type II pairs* of the form $\{x, g(x)\}$ if $\text{dist}[x, g(x)] = \text{dist}[y, g(y)]$ for at least some points and elements g of Γ .

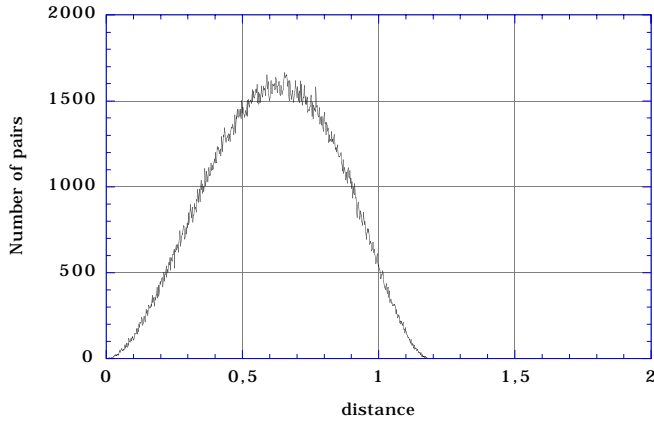


Fig. 8. Pair histogram for a galaxy cluster catalog ($z = 1$) measured by an observer located near a face of the Weeks fundamental domain. Its Klein coordinates are $x = (0, 0, \tanh 0.5)$ and $\Omega_{m0} = 0.2$.

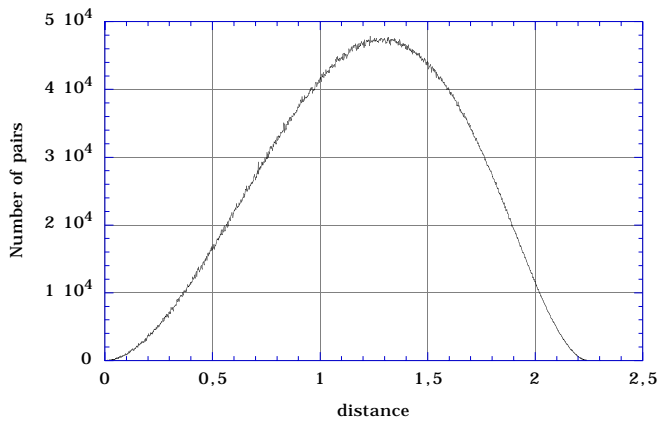


Fig. 9. Pair histogram for a quasar catalog ($z = 3$) measured by an observer centered in $\chi = 0$ in an universe whose spatial sections have the topology of the Weeks manifold and $\Omega_{m0} = 0.2$.

Type I pairs are always present, whatever the topology. Their number roughly equals the number of copies of the fundamental domain within the catalog's limits. Type II pairs produce peaks when the separation distance between topological images is independent of the location of the source.

In compact locally Euclidean universes, type I and type II pairs are both present. The reason is that the 3-torus has the very special property that the separation distance of gg -pairs (i.e. any pair of images comprising an original and one of its ghosts, or two ghosts of the same object) is independent of the location of the source. In other Euclidean spaces the spectrum of gg -pair distances varies with the location of the source. However all closed Euclidean 3-manifolds have the 3-torus as a covering space, so for each such manifold there will be some distances which are independent of the location of the source. As a consequence, the topological signal expected in the histogram from type I and type II pairs clearly stands out, as was shown in the simulations of Lehoucq et al. (1996).

In compact hyperbolic manifolds, $\text{dist}[x, g(x)]$ always depends on the position x of the source (Thurston 1979, 1997). This fact is clearly illustrated by the numerical calculation of

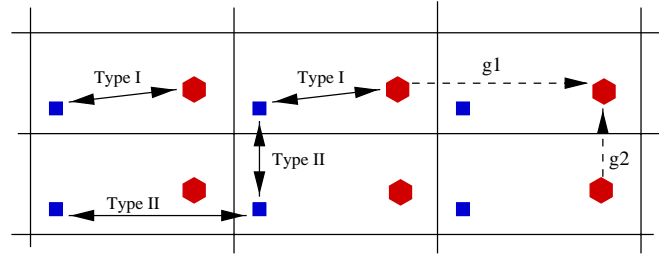


Fig. 10. The difference between type I and type II pairs on the example of the two dimensional torus (the translations g_1, g_2, g_1^{-1} and g_2^{-1} are the generators of its holonomy group). Type I pairs are the ones between the ghosts of two distinct objects and type II pairs are the ones between two topological images of the same object (hexagon or square).

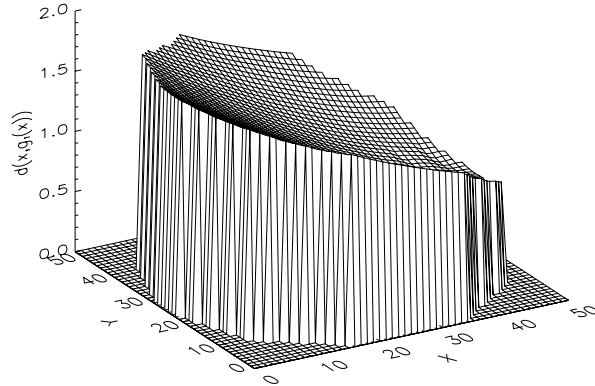


Fig. 11. The function $\text{dist}[x, g_1(x)]$ for all the points located within the fundamental domain of Weeks manifold and on the disk $\varphi = 0$ for the generator g_1 given in Appendix A. This illustrates the fact that this function depends on x in a locally hyperbolic manifold, contrary to Euclidean manifolds.

Fig. 11. Thus type II pairs cannot appear (see Fig. 10). Moreover, as shown in Sect. 3.1, the number of type I pairs is too low to generate significant peaks in the distance histogram. Hence the crystallographic method fails.

The small number of type I pairs in hyperbolic manifolds is due to the rigidity theorem which impose the volume of the manifold once the topology is determined contrary to Euclidean spaces where the characteristic sizes and the volume of the fundamental polyhedron can be chosen at will (since $K = 0$ the geometry does not impose any characteristic size).

In elliptic spaces, distances are position independent whenever the holonomy is a Clifford translation (Weeks, private communication). A Clifford translation is an isometry g such that the displacement function $\text{dist}(x, g(x))$ is constant. This is precisely what is required to get type II pairs in the histogram. All finite groups of Clifford translations of spheres are the cyclic group, the binary dihedral, tetrahedral, octahedral and icosahedral groups (Wolf 1984). Next (theorem 7.6.7 in Wolf 1984): S^3/Γ is a Riemannian homogeneous elliptic space if and only if Γ is a group of Clifford translations of S^3 . Given the classification of three-dimensional spherical space forms (see Sect. 7 of Lachièze-Rey & Luminet 1995), we deduce that all homogeneous elliptic spaces usable for cosmology, such as lens spaces

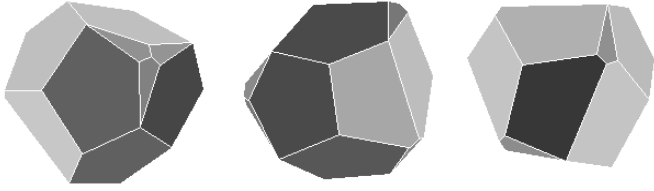


Fig. A1. Three views of the fundamental domain of the Weeks manifold.

Table A1. Klein coordinates of the 26 vertices as defined in Eq. (5).

label	X_1	X_2	X_3
0	0.10797407	0.34689848	-0.41772745
1	-0.00056561	-0.36314169	-0.51501423
2	0.03670097	-0.29313316	-0.54565764
3	-0.08402116	-0.35849225	-0.49943971
4	-0.23493634	0.01568564	-0.59147636
5	-0.08019087	0.60971881	0.08263574
6	0.00049690	0.31902895	0.45245272
7	-0.42135580	-0.01132323	0.46844736
8	-0.44370265	0.45474638	-0.04023802
9	-0.03061224	0.62921121	0.01637099
10	-0.06244403	0.61432068	-0.06105007
11	0.52204774	0.13760656	-0.30585432
12	-0.51128589	0.15380739	-0.31614284
13	-0.50817234	-0.21892234	-0.01808485
14	0.04566464	-0.41129238	-0.46235223
15	-0.18945313	-0.58387452	-0.16877044
16	-0.34964269	0.00034506	0.51260720
17	-0.43363513	-0.08848249	0.43491114
18	-0.11977854	-0.34363564	0.52235338
19	-0.01122014	-0.58564972	0.20470658
20	0.56409719	0.28438251	0.07878044
21	0.43096130	0.11398724	0.43161967
22	0.45298033	0.03203520	0.43691467
23	0.49689789	-0.00018511	0.37162982
24	0.39981755	-0.37241380	0.08914633
25	0.42311163	-0.25223127	-0.40328816

$L(p) = S^3/Z_p$ or the Poincaré dodecahedral space, satisfy this property. The covering transformations which take a point to its nearest neighbours are Clifford translations (although the transformations to more distant neighbours might not be), and type II pairs can be produced.

5. Conclusion

In this article, we generalised the crystallographic method based on the existence of topological images, to universes with non-Euclidean compact spatial sections.

The analysis was performed with the smallest known compact hyperbolic manifold, where we expect to have the greatest number of topological images. It turns out that we do not observe, contrary to Euclidean universes, any peaks in the pair 3D separation histogram.

The absence of peaks is due to combined effects, of the mathematics and of the cosmological parameters.

Table A2. The 18 faces defined by their vertices.

Faces	Labels of vertices				
I	23	24	25	11	20
II	2	4	0	11	25
III	22	18	19	24	23
IV	10	0	4	12	8
V	8	7	16	6	5
VI	15	13	12	4	3
VII	17	13	15	19	18
VIII	14	25	24	19	15
IX	18	22	21	6	16
X	9	20	11	0	10
XI	7	8	12	13	17
XII	5	6	21	20	9
XIII	3	4	2	1	-
XIV	20	21	22	23	-
XV	7	17	18	16	-
XVI	1	2	25	14	-
XVII	1	14	15	3	-
XVIII	10	8	5	9	-

- In locally hyperbolic manifolds $\text{dist}[x, g_n(x)]$ depends on x , so that there is no amplification for the type II pairs $\{x, g_n(x)\}$, whereas $\text{dist}[x, g_n(x)] = \text{dist}[y, g_n(y)]$ in the Euclidean case. This suppresses the peaks.
- The peaks associated to the isometries (i.e. such that $\forall g \in \Gamma, \text{dist}[g(x), g(y)] = \text{dist}[x, y]$) must remain. But, given the cosmological parameters, we have shown in Sect. 3.1 that the number of topological images is too low to create such peaks associated to type I pairs.

In elliptic universes, we have studied the influence of the cosmological parameters. As in the hyperbolic case, type I pairs can be observed for very small universes only and, as in the Euclidean case, type II pairs may be present, due to the fact that the holonomies are Clifford translations. However, such universes are not favored by the present estimates of the cosmological parameters (Proceedings of the “XXIIIrd rencontres de Moriond”).

We conclude that in practice, the crystallographic method will be able to detect the topology only if the universe is locally Euclidean. Such universes have the interesting property that the characteristic sizes of their fundamental domain are decoupled from the cosmological parameters and thus from the Hubble radius. Whatever the underlying geometry, discrete sources such as quasars, X-ray galaxy clusters or infrared galaxies can still help to investigate the cosmic topology by looking for multiple images of individual objects.

Acknowledgements. We are grateful to J. Weeks and H. Fagundes for their precious comments.

Appendix A: description of the Weeks manifold

We considered the Weeks manifold [closed census m003(-3,1)]. Its fundamental polyhedron has 18 faces and 26 vertices (see Fig. A1 and Tables A1 and A2). All the following quantities are

Table A3. Nine generators of the holonomy group. The nine other generators are defined by $g_{k+9} = g_k^{-1}$ and any element $g \in \Gamma$ can be written as $g = \prod_{i \in I} g_{n_i}$; $n_i \in \{1, \dots, 18\}$.

$g_1 =$	$\begin{pmatrix} 1.58926252069783 & -0.40490373463745 & -0.18520828837947 & 1.15217455938197 \\ 1.19813100468664 & -0.37867518857251 & -0.43845341527127 & 1.44909682512520 \\ -0.29994054013040 & 0.58749594014885 & -0.79530849910863 & -0.33510780230833 \\ -0.01652657525663 & 0.82182763167926 & 0.45776096815586 & 0.33959883323000 \end{pmatrix}$
$g_2 =$	$\begin{pmatrix} 1.58926252069784 & 0.58852165407720 & -0.78772550995989 & -0.74758688012532 \\ 0.60542090101752 & 0.63256516975419 & -0.95802870162689 & 0.22040140712305 \\ -0.74661392026174 & -0.95121865744570 & 0.02947692798603 & 0.80730819540762 \\ 0.77575031187707 & -0.20347508215704 & -0.83774912510678 & -0.92658666119331 \end{pmatrix}$
$g_3 =$	$\begin{pmatrix} 1.58926252069784 & 0.90966168251236 & 0.52649891309985 & 0.64889897331428 \\ -0.39527310953786 & -0.96583883836601 & -0.09504624064542 & 0.46299285260867 \\ 0.83783613378036 & 0.46865953388686 & 1.11407913829435 & 0.49107565810403 \\ -0.81703435760262 & -0.82158259245920 & 0.16430152540933 & -0.98262515437950 \end{pmatrix}$
$g_4 =$	$\begin{pmatrix} 1.58926252069784 & -0.50251081201258 & 1.10144921603985 & 0.24504666492427 \\ -0.80335677967765 & 0.05959497029949 & -0.93768098628153 & -0.87326108520599 \\ -0.85819691489983 & 0.41642334058451 & -1.15485297933977 & 0.47896570051526 \\ 0.37930370351109 & -1.03709071788392 & 0.01610402406107 & 0.26087315458913 \end{pmatrix}$
$g_5 =$	$\begin{pmatrix} 1.58926252069784 & -0.11125231907787 & -0.10906253703873 & -1.22535041690502 \\ 0.61314085066332 & -0.72730066360826 & -0.62733910551353 & -0.67336549819589 \\ 0.97779233966538 & 0.49501806133898 & -0.13277443919182 & -1.30130931248255 \\ -0.44015428821540 & 0.48822939502184 & -0.77505563153628 & 0.59553053934699 \end{pmatrix}$
$g_6 =$	$\begin{pmatrix} 1.58926252069784 & -0.48013536446388 & -0.94330313872012 & -0.63671389176518 \\ -1.21801166215147 & 0.63453136165388 & 1.27966469214643 & 0.66586833224629 \\ 0.12199830361655 & 0.75940754853765 & -0.15821652454111 & -0.64276845961162 \\ 0.16528570559051 & -0.50119865773022 & 0.47670391078232 & -0.74085940056587 \end{pmatrix}$
$g_7 =$	$\begin{pmatrix} 2.07713761580105 & -1.55800356296413 & -0.47129628725962 & -0.81547862165852 \\ -0.34790844003080 & 0.59158539050820 & -0.84366445697397 & 0.24351035382656 \\ -0.55790510170459 & 0.95617333032507 & 0.27707820937007 & -0.56587837100861 \\ -1.69770500671437 & 1.47075980034853 & 0.65846650660136 & 1.13379440781211 \end{pmatrix}$
$g_8 =$	$\begin{pmatrix} 2.07713761580106 & -0.62403517630796 & 0.95362111998219 & 1.41974910925485 \\ -0.85113707827869 & 0.92242574522307 & 0.12808289744563 & -0.92582927257265 \\ -0.52567197801091 & -0.52156865254264 & 0.00566611122130 & -1.00213026315664 \\ 1.52109674922046 & -0.51625263825403 & 1.37584734147421 & 1.07436615124600 \end{pmatrix}$
$g_9 =$	$\begin{pmatrix} 2.07713761580107 & 0.70433686017330 & -1.67848312773007 & 0.03323631000097 \\ -0.28072927025369 & 0.14834866484720 & 0.42816244471325 & 0.93460072638127 \\ -1.44346161316703 & -0.14613011383240 & 1.71843229305311 & -0.33048127437171 \\ -1.07336402171483 & -1.20529211233965 & 0.82521087317360 & 0.13567704979006 \end{pmatrix}$

needed to perform our computation and can be obtained from the software *SnapPea*. The volume of the manifold is 0.94272 in units of the curvature radius.

References

- Best L.A., 1971, Canadian J. Math. 23, 451
 Cornish N.J., Spergel D.N., Starkman G.D., 1998a, Phys. Rev. D57, 5982
 Cornish N.J., Spergel D.N., Starkman G.D., 1998b, Proc. Nat. Acad. Sci. 95, 82
 Cornish N.J., Spergel D.N., Starkman G.D., 1998c, Class. Quant. Grav. 15
 Coxeter H.S.M., 1965, Non Euclidean geometry. University of Toronto Press
 Proceedings of the workshop: Cosmology and topology. Cleveland 25-27 october 1997, Class. Quant. Grav. 15, 1998
 Demianski M., Lapucha M., 1987, MNRAS 224, 527
 Ellis G.F.R., 1971, Gen. Rel. Grav. 2, 7
 Fagundes H.V., 1985, ApJ 291, 450
 Fagundes H.V., Wichoski W.F., 1987, ApJ 322, L5
 Fagundes H.V., 1989, ApJ 338, 618
 Fagundes H.V., 1990, ApJ 349, 678
 Fagundes H.V., 1993, Phys. Rev. Lett. 70, 1579
 Fagundes H.V., Gaussman E., 1997, astro-ph/9704259
 Fang L.Z., Sato H., 1983, Comm. Theoret. Phys. China 2, 1055
 Gabai D., Meyerhoff G.R., Thurston N., 1996, MSRI preprint 1996-058
 Gott J.R., 1980, MNRAS 193, 153

- Gradshteyn I.S., Ryzhik I.M., 1980, Table of integrals series and products. ed. Academic N.Y.
- Hawking S., Ellis G.F.R., 1973, Large scale structure of spacetime. Cambridge University Press
- Lehoucq R., Lachièze-Rey M., Luminet J.-P., 1996, A&A 313, 339
- Lachièze-Rey M., Luminet J.-P., 1995, Phys. Rep. 254,135
- Matveev S.V., Fomenko A.T., 1988, Russian Math. Surveys 43, 3
- Misner C.W., Thorne K.S., Wheeler J.A., 1973, Gravitation. San Francisco, Freeman
- Proceedings of the “XXIIIrd rencontres de Moriond: Fundamental Parameters in Cosmology”, Eds. Trân Thanh Vân (1998)
- Mostow G.D., 1973, Ann. Math. Studies 78, Princeton University Press
- de Oliveira Costa A., Smoot G.F., Starobinsky A.A., 1996, ApJ 468, 457
- Paál G., 1971, Acta. Phys. Acad. Hungaricae 30, 51
- Peebles P.J.E., 1993, Principles of Physical Cosmology. Princeton University Press
- Prasad G., 1973, Invent. Math. 21, 255
- Roukema B.F., 1996, MNRAS 283, 1147
- Roukema B.F., Edge A.C., 1997, MNRAS 292, 105
- Spergel D., Proceedings of the workshop: Cosmology and topology. Cleveland 25-27 october 1997, Class. Quant. Grav. 15, 1998
- Stevens D., Scott D., Silk J., 1993, Phys. Rev. Lett. 71, 20
- Thurston W.P., 1979, The topology and geometry of three manifolds. Princeton Lecture Note
- Thurston W.P., 1997, In: Levy S. (ed.) Three Dimensional Geometry and Topology. Princeton University Press
- Uzan J.P., 1998a, Phys. Rev. D58, 087301
- Uzan J.P., 1998b, Class. Quant. Grav. 15, 2711
- Weeks J., 1985, Ph.D. Thesis, Princeton University
- Wolf J.A., 1984, Spaces of constant curvature. 5th edition, Publish or Perish Inc., Wilmington USA